View metadata, citation and similar papers at core.ac.uk

brought to you by CORE

provided by City Research Online

Read, M. G., Smith, I.K. & Stosic, N. (2017). Optimisation of power generation cycles using saturated liquid expansion to maximise heat recovery. Proceedings of the Institution of Mechanical Engineers, Part E: Journal of Process Mechanical Engineering, 231(1), pp. 57-69. doi: 10.1177/0954408916679202

CITY UNIVERSITY LONDON

City Research Online

Original citation: Read, M. G., Smith, I.K. & Stosic, N. (2017). Optimisation of power generation cycles using saturated liquid expansion to maximise heat recovery. Proceedings of the Institution of Mechanical Engineers, Part E: Journal of Process Mechanical Engineering, 231(1), pp. 57-69. doi: 10.1177/0954408916679202

Permanent City Research Online URL: http://openaccess.city.ac.uk/16082/

Copyright & reuse

City University London has developed City Research Online so that its users may access the research outputs of City University London's staff. Copyright © and Moral Rights for this paper are retained by the individual author(s) and/ or other copyright holders. All material in City Research Online is checked for eligibility for copyright before being made available in the live archive. URLs from City Research Online may be freely distributed and linked to from other web pages.

Versions of research

The version in City Research Online may differ from the final published version. Users are advised to check the Permanent City Research Online URL above for the status of the paper.

Enquiries

If you have any enquiries about any aspect of City Research Online, or if you wish to make contact with the author(s) of this paper, please email the team at publications@city.ac.uk.

Optimisation of power generation cycles using saturated liquid expansion to maximise heat recovery

M.G. Read, I.K. Smith and N. Stosic

Centre for Compressor Technology, City University London, Northampton Square, London, UK
Email: m.read@city.ac.uk

Nomenclature:

HP	High pressure
LP	Low pressure
ORC	Organic Rankine Cycle
TFC	Trilateral Flash Cycle
BIVR	Built-In Volume Ratio
V	Volume
η	Efficiency
P	Power
Q	Heat transfer rate
$\dot{m}$	Mass flow rate
h	Enthalpy
p	Pressure

Subscripts:

$down$	downstream of the expander stage
up	upstream of the expander stage
wc	working chamber of the twin-screw expander stage
suc	relating to the twin-screw rotor position at which the suction port opens
dis	relating to the twin-screw rotor position at which the discharge port opens

Abstract

The use of two-phase screw expanders in power generation cycles can achieve an increase in the utilisation of available energy from a low temperature heat source when compared with more conventional single-phase turbines. The efficiency of screw expander machines is sensitive to expansion volume ratio, which, for given inlet and discharge pressures, increases as the expander inlet vapour dryness fraction decreases. For single-stage screw machines with low inlet dryness, this can lead to under expansion of the working fluid and low isentropic efficiency for the expansion process. The cycle efficiency can potentially be improved by using a two-stage expander, consisting of a low pressure machine and a smaller high pressure machine connected in series. By expanding the working fluid over two stages, the built-in volume ratios of the two machines can be selected to provide a better match with the overall expansion process. This increases the efficiency for particular inlet and discharge conditions. The mass flow rate though both stages must be matched, and the compromise between increasing efficiency and maximising power output must also be considered. This study is based on the use of a rigorous thermodynamic screw machine model to compare the performance of single and two-stage expanders. The model allows optimisation of the required intermediate pressure in the two-stage expander, along with the built-in volume ratio of both screw machine stages. The results allow the two-stage machine, using either two screw machines or a combination of high pressure screw and low pressure turbine, to be fully specified in order to achieve maximum efficiency for a specified power output. It is shown that for the low temperature heat recovery application considered in this paper, the

TFC using a two-stage expander and the Smith Cycle using a high pressure screw and low pressure turbine are both predicted to achieve a similar overall conversion efficiency to that of a conventional saturated vapour ORC.

1. Introduction

Organic Rankine Cycle (ORC) systems can be used to recover power from low temperature heat sources but the cycle efficiencies attainable from them are much lower than those associated with conventional high temperature steam plant, while the required surface area of the heat exchangers per unit power output is much higher. The lower latent heat of evaporation of organic fluids relative to steam also means that the feed pump work required in ORCs is a significantly higher proportion of the gross power output.

For low source temperatures, the power generation cycle normally considered is that where the working fluid enters the expander as dry saturated vapour, as shown in Figure 1. However, in most cases, this leads to the working fluid leaving the expander with some superheat, which must be removed before condensation begins.

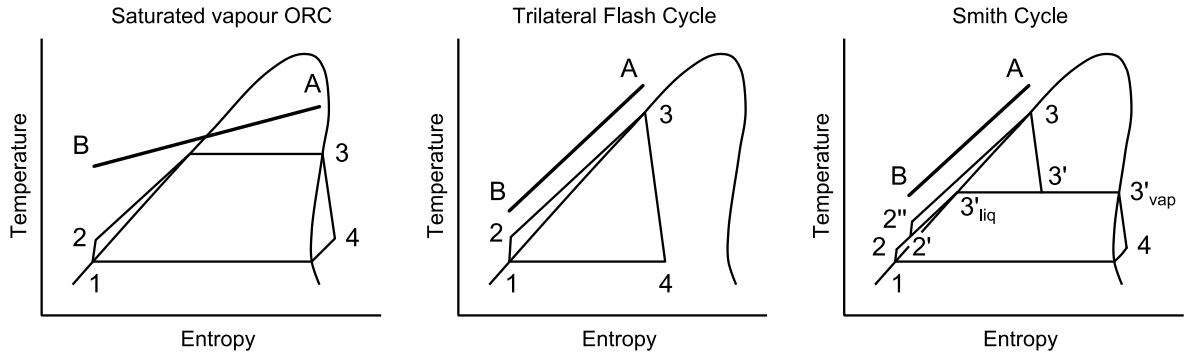

Figure 1: Illustrative T-s diagrams showing conventional ORC with saturated vapour at the expander inlet, TFC with saturated liquid at the expander inlet and a Smith Cycle with direct contact feed heating

Maximising net power output from the cycle is a compromise between increasing the mean temperature of heat addition (which, in accordance with Carnot's principle, increases cycle efficiency) and increasing the amount of heat extracted from the source, which requires a lower evaporation temperature. This can be achieved in a Trilateral Flash Cycle (TFC) which expands the working fluid from a saturated liquid state as shown in Figure 1. Although this system has been considered for many years [1-3], to date, no large scale demonstration unit of it is known to have been built. This is because of the lack of suitable two-phase expanders with adiabatic efficiencies approaching those of dry vapour turbines. By the use of a screw expander, instead of the more conventional turbine, it is possible to admit the working fluid to the expander as wet vapour and thereby eliminate both the need to desuperheat the vapour after expansion and simultaneously to raise the evaporation temperature, thus improving the cycle efficiency. The potential cost and performance benefits of using screw expanders in ORC systems have been extensively studied for geothermal applications [4-6]. A major issue with using positive displacement expanders such as screw machines is the inherent limitation on expansion volume ratio that can be achieved. The Smith Cycle [7] has previously been proposed as an alternative cycle capable of maximizing heat recovery from the source. This is achieved via a high pressure saturated liquid expansion stage, while separation of the 2-phase working fluid at an intermediate pressure limits the required volume ratio for the high pressure expansion and allows the use of a turbine for the low pressure

stage, which is better suited to the higher volume flow rates. The Smith Cycle can be implemented with direct (as shown in Figure 1) or indirect feed heating, or with no feed heating as discussed in Section 5.

In the fields of geothermal and waste heat recovery systems, there is growing interest in generating power from heat sources with initial temperatures in the 170-200°C range. At these temperatures, simple ORC systems are less attractive, as their use under these circumstances requires either a multi-stage turbine to accommodate the large pressure ratio, or a cascade arrangement of two cycles containing different working fluids [8]. In the cascade arrangement, one cycle operates over a higher temperature range and the condenser of this unit acts as the evaporator of the second unit with different working fluids in each closed loop. Alternatively, Kalina type systems, which require at least three heat exchangers, may be suitable [9]. As these systems are relatively complex, this study aims to re-examine the possibility of using systems incorporating saturated liquid expansion for power recovery from higher temperature resources. While earlier studies have investigated these cycles using simple assumptions regarding the performance of the 2-phase expander, here a detailed thermodynamic model of twin-screw positive displacement machines has been used to assess the efficiency and power limitations of practical single and two-stage expanders in TFC and Smith Cycle applications.

At resource temperatures in the 170-200°C range, a suitable working fluid for a TFC system is pure n-pentane. With such a working fluid, a volume ratio of expansion of the order of 160:1 occurs during the expansion process. When using twin-screw machines, where the built-in volume ratio is limited by geometrical and performance considerations, a two stage expander is required to achieve efficient expansion. The design of the first and second stage expanders must therefore be optimised for the admission of saturated liquid and wet vapour respectively. Likewise, the performance of the Smith Cycle is dependent on optimizing the operation of the high pressure expander. While previous work has studied the performance of combined twin-screw and turbine systems [6, 7], recent progress in developing and validating a computational twin-screw model has allowed the performance of single and two-stage systems to be investigated in greater detail. This model allows the optimisation of the expander parameters for a particular application, and can be incorporated with other detailed component models to allow multi-variable optimisation of low temperature heat recovery systems.

2. Twin-screw expander model

The main aspects of a detailed computational model for screw machines were established by Taniguchi et al. [10], and developments in numerical methods have allowed the investigation of rotor profiles and machine geometries for a range of applications [11-13]. The full thermodynamic model of the expander used to investigate the performance of screw machines in the current study is based on the quasi one dimensional analysis of twin-screw machines as described by Stosic and Hanjalic [14, 15], which has been extensively validated for compressors for a wide range of working fluids and operating conditions. For expanders, the model has been validated for expansion of low dryness fluid (including saturated liquid) using the refrigerant R113 [16], and more recently for the expansion of high dryness wet steam [17].

The screw expander calculation procedure requires the rotor geometries to be specified in order to calculate machine performance. An initial optimization has therefore been performed to identify suitable rotor profiles for operating conditions representative of the application considered in the current study. The “N” rotor profile developed at City University has been used in the analysis as this geometry is known to have benefits including greater throughput and a stiffer gate rotor than is possible using alternative profiles with similar blow-hole area and sealing line lengths [7]. For the specified geometry, the characteristics of the screw machine such as the working chamber volume as a function of angular position, sealing line lengths, blowhole area and axial/radial clearances between the rotors and the casing are defined as fixed inputs for the expander model, the main elements of which are described.

The working fluid properties throughout the expansion process and the machine performance are calculated by assuming quasi one-dimensional fluid flow through the machine. The internal energy of

the fluid can be found by applying Equation (1) which describes the conservation of internal energy for non-steady flow in a single working chamber of the machine. The total enthalpy of the fluid at the inflow and outflow of the working chamber are function of the angular position of the main rotor, θ, and are shown in Equations 2 and 3:

$$\omega\left(\frac{dU}{d\theta}\right) = \dot{m}_{in}h_{in} - \dot{m}_{out}h_{out} + \dot{Q} - \omega\left(p\frac{dV}{d\theta}\right) \quad (1)$$

$$\dot{m}_{in}h_{in} = \dot{m}_{suc}h_{suc} + \{\dot{m}_{leak}h_{leak}\}_{gain} \quad (2)$$

$$\dot{m}_{out}h_{out} = \dot{m}_{dis}h_{dis} + \{\dot{m}_{leak}h_{leak}\}_{loss} \quad (3)$$

The mass flow rates into and out of the working chamber (via the suction and discharge ports and leakage paths) are also functions of the rotor angle, as shown in Equations 4 and 5, and the mass continuity equation is defined in Equation 6:

$$\dot{m}_{in}(\theta) = \dot{m}_{suc}(\theta) + \{\dot{m}_{leak}(\theta)\}_{gain} \quad (4)$$

$$\dot{m}_{out}(\theta) = \dot{m}_{dis}(\theta) + \{\dot{m}_{leak}(\theta)\}_{loss} \quad (5)$$

$$\omega\left(\frac{dm}{d\theta}\right) = \dot{m}_{suc} + \{\dot{m}_{leak}\}_{gain} - \dot{m}_{dis} - \{\dot{m}_{leak}\}_{loss} \quad (6)$$

The subscripts $gain$ and $loss$ relate to the total mass flow rates of pressure driven leakage flows into and out of the working chamber via the rotor tip, interlobe and end face leakage paths. Characterisation of these leakage flows is achieved by applying the continuity and momentum equations and assuming an isenthalpic throttling process with negligible change in temperature to achieve the expression for leakage mass flow rate given in Equation 7 [14,18]:

$$\dot{m}_{leak} = \mu_{leak}A_{leak}\sqrt{\frac{({p_2}^2 - {p_1}^2)}{RT_2(\zeta + 2\ln(p_2/p_1))}} \quad (7)$$

In Equation 7, μ_{leak} is the leakage flow discharge coefficient (a function of Reynolds and Mach numbers) and ζ is the leakage flow resistance that can be evaluated as a function of the shape and dimensions of the leakage path and the Reynolds number [18]. The viscosity of the fluid in the leakage path is therefore required. The leakage fluid is assumed to be at the same conditions as the working chamber from which it is leaking, and the viscosity can be easily obtained for pure liquid or vapour phase conditions. In the case of 2-phase fluid the assumption in Equation 8 has been applied in order to find an approximate value of dynamic viscosity, υ, as a function of pressure, p, fluid quality, x, and the saturated liquid and vapour viscosities:

$$1/\upsilon_{leak} = x/\upsilon_{vap}(p) + (1-x)/\upsilon_{liq}(p) \quad (8)$$

Using these equations, the thermodynamic processes in the expander can be found by considering the working chamber volume as a function of rotor angle (defined by the specified machine geometry and rotor profiles), and combining with the differential equations for internal energy and working chamber mass balance. The result differential equations are solved using a fourth order Runge-Kutta numerical method. Once the specific internal energy and instantaneous bulk density are known in the working chamber, an equation of state for the working fluid can be used to determine the corresponding temperature, pressure and fluid quality. The mass flow rates into and out of the working chamber depend on the instantaneous chamber mass and internal energy. Once initial conditions are specified as a function of rotor angle, a number of iterations are required to find a converged solution. Once the convergence criteria are satisfied, the indicated power output of the expander can be found by numerical integration of the indicated p-V diagram for the working chamber. The general parameters used to define the screw expanders considered in this study are defined in Table 1.

Parameter	Value
Lobe No. of main/gate rotor	4/5
Maximum BIVR	4.5
Main rotor tip speed	60 m/s
Length/diameter ratio	1.5
Wrap angle	300°
Mechanical efficiency	90%

Table 1: General parameters used for analysis of twin-screw expanders

An important machine parameter is the built-in volume ratio, BIVR, defined in Equation 9 as the ratio of working chamber volumes at discharge port opening and suction port closing.

$$\text{Built-in volume ratio:} \quad BIVR = V_{dis}/V_{suc} \tag{9}$$

Figure 2 illustrates how decreasing the BIVR for a particular machine increases the volume of working fluid admitted through the suction port per revolution. For a particular rotational speed of the machine, the volumetric and mass flow rates can be determined. It is important that the value of BIVR is optimised for particular operating conditions, as over or under expansion of the working fluid, as illustrated in Figure 3, can significantly reduce the expander efficiency.

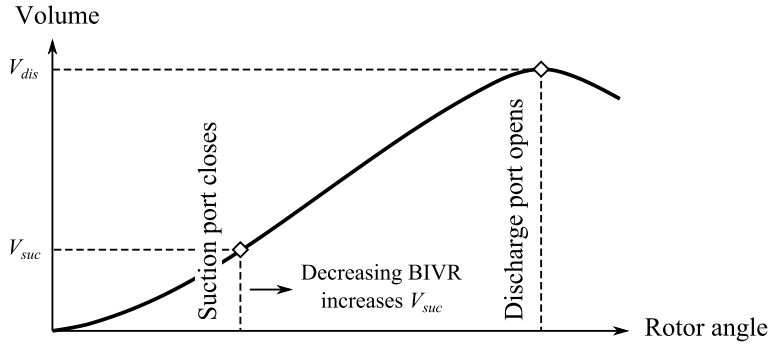

Figure 2: Schematic diagram of working chamber volume as a function of rotor angle

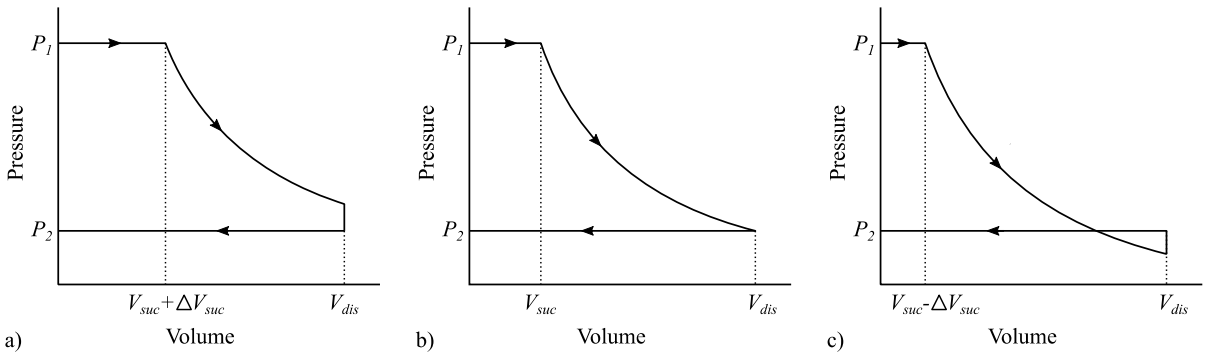

Figure 3: Illustration of a) under expansion, b) full expansion and c) over expansion of the working fluid relative to discharge pressure in an ideal screw expander

For single-stage screw expander machines, the inlet dryness fraction and the pressures at the inlet and discharge are defined by the requirements of the cycle. The variable input parameters required for

the expander model are then limited to the expander size, main rotor speed and BIVR. Two approaches can be taken to match the machine operation to the required cycle conditions:

i. The BIVR is specified and iterations are performed to find the rotor speed required to match the mass flow rate of expander to that of the working fluid required in the cycle – no limits are imposed on rotor speed, which in some cases can become impractically high.

ii. The rotor speed is fixed and iterations are performed to find the value of the BIVR required to match the mass flow rate – if the BIVR is greater than the limit for the chosen screw machine geometry then the expander cannot meet the requirements of the cycle conditions.

For two-stage machines, the intermediate pressure between the two stages is an additional input parameter. There is also an additional constraint, as the mass flow rate through both the high pressure (HP) and low pressure (LP) stages must be the same. While the mass flow rate of the HP stage is largely dependent on the inlet conditions and the size and BIVR of the HP machine, it is to a lesser degree also dependent on the intermediate pressure, as this affects leakage flows in the machine. To characterise the performance of a two-stage expander for particular conditions, the following iterative approach is therefore required:

i. Specify the size, speed and BIVR of both stages.

ii. Estimate the intermediate pressure, and calculate the mass flow rates of the HP and LP stages.

iii. While the difference between the HP and LP mass flow rates is greater than an allowable error, repeat step ii.

iv. While the difference between the converged and required mass flow rates is greater than an allowable error, repeat steps i-iii, fixing either the speed or BIVR of the two stages as required.

The single or overall two-stage expander efficiency calculated using these approaches can be used in a thermodynamic cycle model to calculate overall system performance for specific operating conditions. It is then possible to apply an iterative numerical procedure to identify the optimum operating conditions for the cycle. The program is however computationally intensive, and the focus of this paper is to illustrate how the optimum expander parameters can be selected for specified cycle conditions. An initial optimisation of the Trilateral and Smith cycles has therefore been performed assuming a representative constant expander efficiency in order to identify appropriate overall operating conditions. The full thermodynamic model of the screw expander is then used to assess the performance and the design requirements for single and two-stage expanders operating at the conditions. Results of the TFC are compared with the Smith Cycle and conventional saturated ORC, which are assessed using a representative achievable turbine efficiency. Details of the cycle models are presented below.

3. Modelling of power generation cycles with single and two-stage expanders

The analysis presented in this paper has been performed for a simple heat recovery application from a single phase source fluid, defined as follows;

Assumptions:

Heat Source Inlet Temperature	190°C
Heater Pinch Point Temperature Difference	5°C
Available Cooling Water Temperature	20°C
Condenser Pinch Point Temperature Difference	5°C
Degree of sub-cooling prior to feed pump inlet	2°C

For the proposed TFC and Smith Cycle systems, where expansion must begin from the saturated liquid condition, a suitable working fluid for this case is n-pentane, which has a critical temperature of 196.6°C. For the saturated vapour ORC several working fluids were considered, including the refrigerant R245fa which is commonly used in low temperature heat recovery applications but will be phased out in the near future due to its high global warming potential (GWP). A range of low GWP simple hydrocarbons were therefore also considered. In all cases, the pressure of the working fluid in the condenser was constrained to be greater than or equal to atmospheric, so as to prevent air leaking into system. All thermo-fluid properties were obtained from the 'Reference Fluid Thermodynamic and Transport Properties Database' (REFPROP) program produced by the National Institute of Standards and Technology (NIST), which was integrated with the cycle and expander models. An initial cycle analysis program was used to identify suitable operating conditions for the expander.

3.1. Initial optimisation of TFC, dry saturated ORC and Smith Cycle systems

The aim of this study is to investigate the performance of cycles using screw expanders over a range of possible power outputs. The performance of conventional ORC systems has been include for comparison, but a detailed consideration of turbine design was not considered. A representative achievable turbine efficiency has been selected based on the literature [19,20,21], which indicates that modern design methods can be used to achieve high efficiency of radial flow turbines for organic fluids, even at low power outputs. For specific applications, a more detailed consideration of turbine sizing and performance would be appropriate.

The component efficiencies in Table 1 have been used in order to estimate the performance of the conventional saturated vapour ORC, TFC and Smith Cycle illustrated in Figure 1. A so called 'Flash' cycle, where the 2-phase expander in the Smith Cycle is replaced by a throttle valve, has also been considered for comparison; as the throttling process is isenthalpic, this case is equivalent to a Smith Cycle with the isentropic efficiency of the 2-phase expander equal to zero.

Expander isentropic efficiency, η_{isen}	80% for screw 85% for turbine
Expander mechanical efficiency, η_{mech}	90% for screw 95% for turbine
Pump efficiency	70%
Motor efficiency	90%
Generator efficiency	95%

Table 2: Assumed component efficiencies for initial cycle optimisation

The isentropic and adiabatic efficiency of an expander are defined in Equations 10 and 11. This is an important distinction as the isentropic efficiency of the expander affects the outlet conditions of the working fluid, and hence the performance of other components in the cycle, while the adiabatic efficiency includes the mechanical losses that affect the shaft power output from the machine.

Isentropic expander efficiency: $$\eta_{isen} = (h_{in} - h_{out}) / \left(h_{in} - h_{out,isen}\right) \quad (10)$$

Adiabatic expander efficiency: $$\eta_{adi} = P_{shaft} / \left(\dot{m} h_{in} - \dot{m} h_{out,isen}\right) = \eta_{isen} \eta_{mech} \quad (11)$$

A simple optimization algorithm has been used to identify the cycle conditions that achieve maximum conversion efficiency, defined as the net power output divided by the total available heat from the source fluid. It can be shown that this is the product of the cycle efficiency and the heat recovery efficiency,

as defined in Equations 12-14, where $Q_{source,max}$ is the heat available if the source fluid were cooled to the initial temperature of the sink fluid.

Cycle efficiency: $\eta_{cyc} = P_{net}/Q_{source}$ (12)

Heat recovery efficiency: $\eta_{rec} = Q_{source}/Q_{source,max}$ (13)

Conversion efficiency: $\eta_{conv} = P_{net}/Q_{source,max} = \eta_{cyc}\eta_{rec}$ (14)

An understanding of heat exchanger pressure losses requires a detailed consideration of heat exchanger design and flow conditions which is beyond the scope of this study. To allow a simple comparison of the different proposed cycles the pressure losses have therefore been neglected. The effect of these pressure losses will be considered in future studies, but is not expected to alter the relative performance of the power generation cycles, considered here, significantly. No regenerative or recuperative feed heating has been applied in either saturated vapour ORC or Smith Cycle as no lower temperature limit has been imposed for the heat source. In such cases, preheating the feed liquid reduces the heat input from the source fluid, thereby increasing its exit temperature, but the total heat input, mass flow rate and net power output are essentially unchanged, and the additional system complexity is therefore unnecessary.

Cycle:	**Saturated vapour ORC**				
Working fluid	n-Pentane	Isopentane	Neopentane	n-Butane	R245fa
GWP (100 year) [22]	~20	~20	~20	~20	1030
Critical temperature (°C)	196.6	187.2	160.6	152.0	154.0
Expander inlet temp. (°C)	119.2	121.0	138.9*	130.7*	132.6*
Condenser saturation temp. (°C)	36.0	29.0	29.1	29.0	29.0
Expansion pressure ratio	8.8	10.5	11.6	9.7	14.4
Expansion volume ratio	9.4	11.6	16.2	12.9	18.8
Source fluid exit temp. (°C)	71.0	62.1	51.1	49.8	50.1
Cycle efficiency	12.1%	12.3%	12.6%	12.7%	12.9%
Heat recovery efficiency	70.0%	75.2%	81.7%	82.5%	82.3%
Conversion efficiency	8.5%	9.3%	10.3%	10.4%	10.6%

Table 3: Results of initial cycle optimization of the saturated vapour ORC to achieve maximum conversion efficiency using a range of working fluids (recuperation is not applied, * indicates evaporation temperature is limited to 95% of critical temperature)

Cycle:	**TFC**	**Smith**	**Flash**
η_{isen} for saturated liquid expansion	80%	80%	0%
HP expander inlet temperature (°C)	175.0	175.0	175.0
Separator saturation temperature (°C)	-	73.7	116.7
Condenser saturation temperature (°C)	36.0	36.0	36.0
Source fluid exit temperature (°C)	46.0	45.8	45.8
LP expander pressure ratio	-	3.1	8.5
Cycle efficiency	11.5%	12.1 %	8.7%
Heat recovery efficiency	85%	85%	85%
Conversion efficiency	9.7%	10.3%	7.4%

Table 4: Results of initial optimisation of cycles incorporating saturated liquid expansion using n-pentane working fluid (no recuperation or regeneration is applied)

These initial results show that the selection of working fluid is an important factor in the performance of the saturated vapour ORC. The results in Table 3 show that there is significant variation in the required pressure and volume ratios, and the practicality of designing turbines for these operating conditions must be considered for specific applications, as this will influence the size, performance and cost of the turbine. A detailed discussion of turbine design issues for a similar waste heat recovery application can be found in Uusitalo [19]. The results in Table 3 are however considered to provide a good indication of the potential performance of conventional saturated vapour ORCs. The results for the cycles incorporating saturated liquid expansion, shown in Table 4, are seen to achieve similar performance in terms of the overall conversion efficiency. This occurs as a result of the greater heat recovery from the source fluid, which to a large degree offsets the slightly lower cycle efficiency caused by the lower efficiency of the screw expander. More detailed analysis of the screw expander components is however required to assess the performance and power output of TFC and Smith Cycle systems using practical screw machines. Rather than specify the heat input to the cycle, and thereby determine a required mass flow rate for the working fluid, it is useful to characterise the performance of a range of single and two-stage expanders as a function of mass flow rate at these conditions. Standard twin-screw machine sizes, with main rotor diameters ranging from 145-408mm, have been analysed in order to illustrate what is achievable with practical single and two-stage expanders. To identify the maximum mass flow rates possible with these machines, and to ensure high efficiency, the performance has been considered at maximum allowable rotational speeds corresponding to a main rotor tip speed of 60m/s. All expander sizes are defined by the main rotor diameter, and have the general characteristics shown in Table 1.

4. Results of TFC expander modelling

For the application specified above, a two-stage expander for the TFC requires a relatively small HP machine in comparison with the size of the LP machine, due to the much higher density of the fluid at the HP inlet. A combination of a 145mm HP machine with a 408mm LP machine has been found to achieve good overall performance with well-matched expansion in both stages. The mass flow rate, overall adiabatic efficiency, required intermediate pressure and total shaft power are all dependent on the BIVRs of the HP and LP machines. The overall performance of the two-stage machine has therefore been calculated over a range of BIVR values, and contour maps of the key results are shown in Figures 4-6.

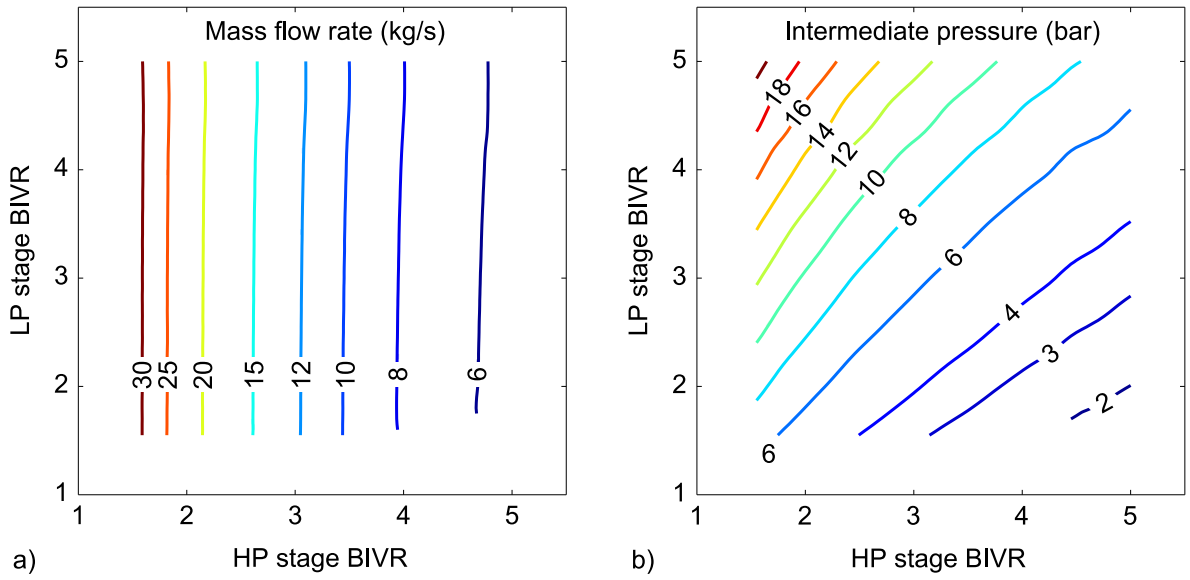

Figure 4: Contour maps showing a) mass flow rate (kg/s) and b) intermediate pressure (bar) of the 2-stage screw expander consisting of 145mm and 408mm machines

The results in Figure 4 show that mass flow rate is, as expected, very strongly dependent on the BIVR of the HP stage. Increasing the BIVR of the LP stage increases the required intermediate pressure, but causes only a small change in mass flow rate due to the reduction in leakage flow. The performance of the 2-stage screw machine can be understood by examining the isentropic efficiency achieved in each stage and relating this to the degree of under or over expansion of the working fluid in the machines. To illustrated this, a discharge pressure ratio, R_{dis}, has been defined as shown in Equation 1, quantifying the difference between the downstream pressure and the pressure of the expanded fluid in the screw machine, at the point where the discharge port opens, as a proportion of the upstream pressure.

$$\text{Discharge pressure ratio:} \quad R_{dis} = \frac{p_{wc,dis} - p_{down}}{p_{up}} \tag{1}$$

Using this definition, positive and negative values of R_{dis} relate to under and over expansion respectively. The values obtained for the discharge pressure ratio and the isentropic efficiency of both stages of the 2-stage machine are shown in Figures 5 and 6 respectively.

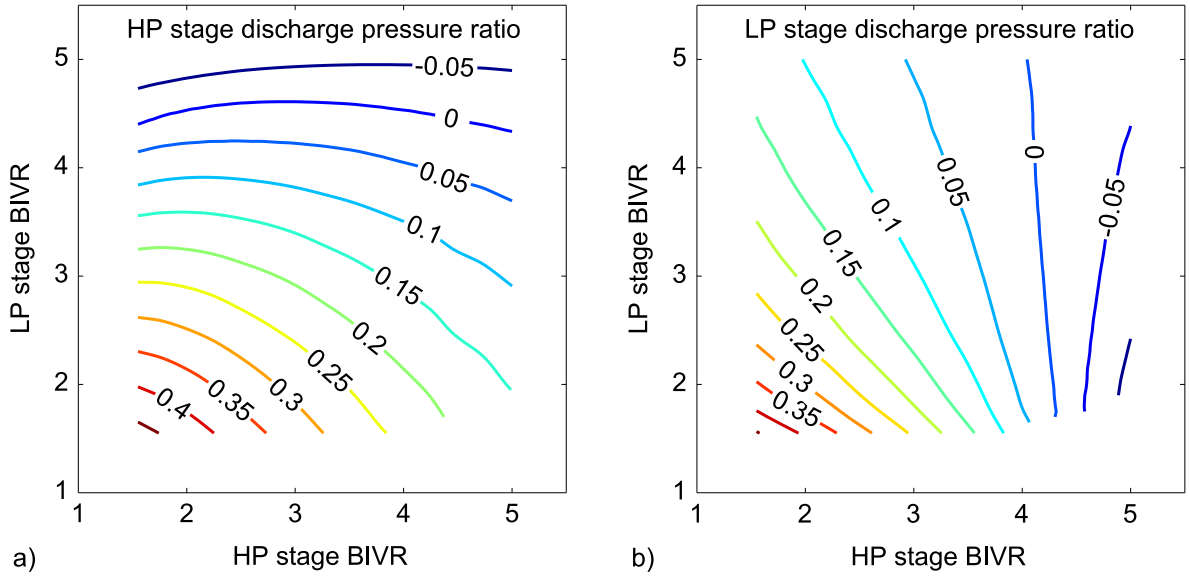

Figure 5: Discharge pressure ratio, R_{dis}, for the a) 145mm high pressure stage and b) 408mm low pressure stage of the 2-stage screw expander

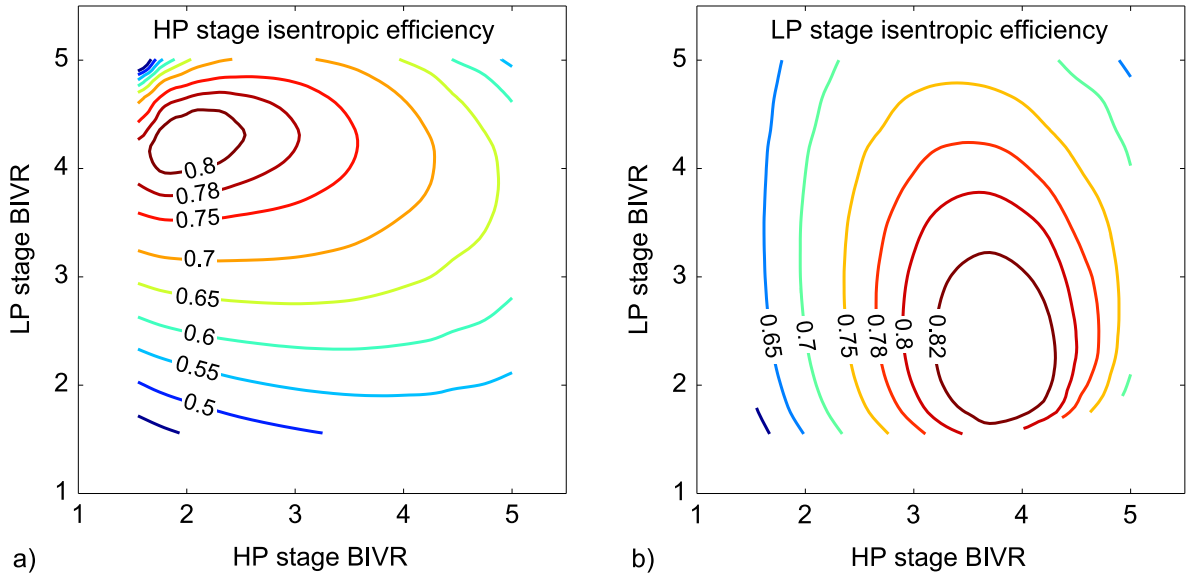

Figure 6: Isentropic efficiency for the a) 145mm high pressure stage and b) 408mm low pressure stage of the 2-stage screw expander

From Figures 5 and 6 it can be seen that for both the high and low pressure stages, the maximum efficiency for a given BIVR is achieved when R_{dis} is around 5%, and the working fluid is therefore slightly under-expanded. In each stage, the maximum efficiency is seen to fall as the associated BIVR increases, due to the increase in the leakage flows as a proportion of the overall mass flow rate. When considering the overall performance of the 2-stage machine it is clear that there is a compromise between maximizing the efficiency of the two stages, which will depend on the power output from both. This is seen in Figure 7, where the performance of the two expander stages has been used to calculate the total shaft power output and the overall adiabatic efficiency of the 2-stage machine.

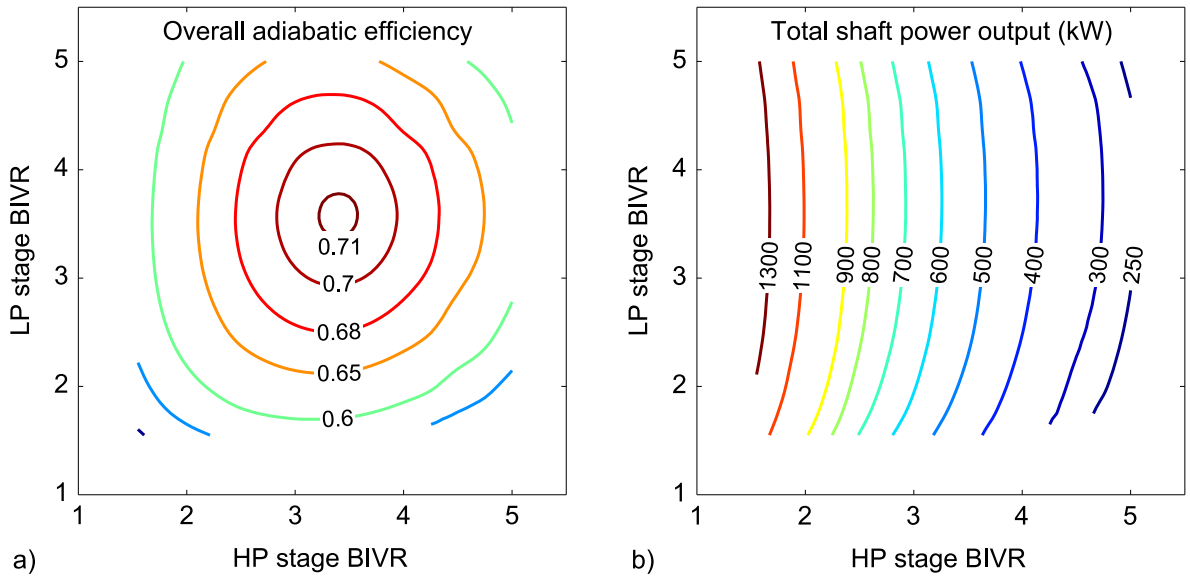

Figure 7: Contour maps showing; a) overall adiabatic efficiency; b) total shaft power (kW) of 2-stage screw expander

Figure 7 shows that the maximum overall adiabatic efficiency occurs at BIVR values of 3.4 and 3.6 for the HP and LP stages respectively. This corresponds to an intermediate pressure of 6.9 bar, mass flow rate of 9.9 kg/s and total shaft power of 520 kW. For a fixed HP BIVR, it can be seen that the required intermediate pressure increases as the LP BIVR increases. The maximum efficiency point corresponds to the case when the BIVRs of both stages are well matched to the expansion, but at lower values of LP BIVR, the intermediate pressure falls, leading to increased under-expansion for the HP, and to a lesser extent LP, stages. Conversely, at higher values of LP BIVR the rise in intermediate pressure can lead to over-expansion for the HP stage and under-expansion for the LP stage. In conclusion, the circular overall efficiency contours are a result of over or under expansion leading to a reduction in efficiency in one or both of the expander stages.

The results for the two stage expander allow a full cycle analysis to be performed to find the net power output including feed pump and condenser pump power consumption. Other than the calculated efficiency of the 2-stage expander, the assumptions described in Section 3 are used to characterise the cycle.

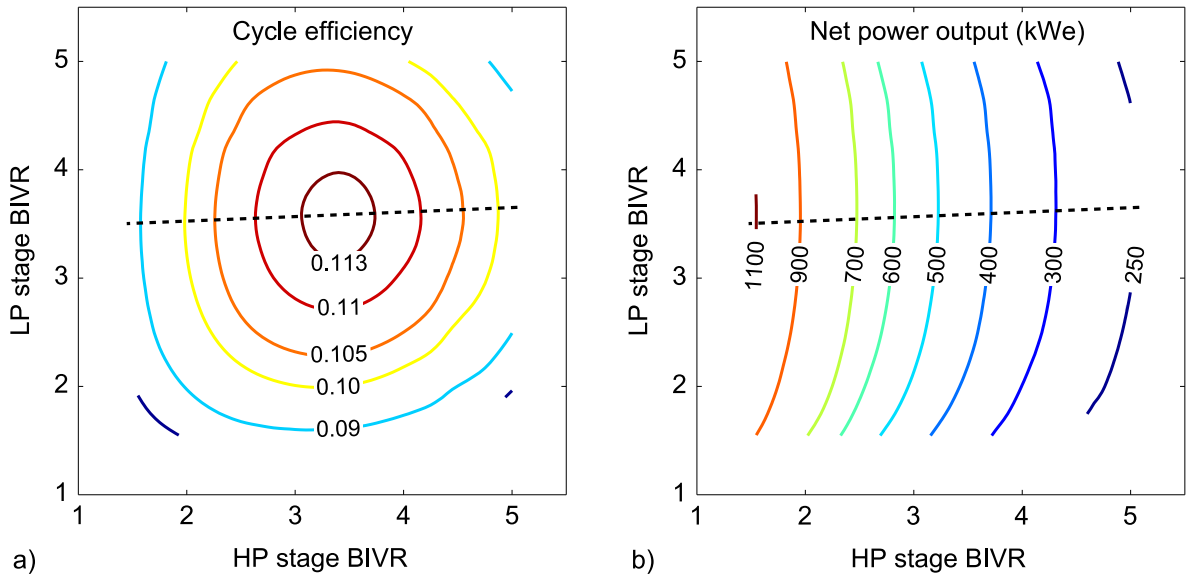

Figure 8: Contour maps showing; a) Cycle efficiency; b) Net power output (kWe) for the TFC with 2-stage screw expander, where dashed lines shows contour of maximum cycle efficiency as a function of net power output

In Figure 8, the maximum cycle efficiency is seen to occur at the same conditions as maximum overall expander efficiency, with a corresponding net power output of around 500kWe. The net power output is however shown to increase as the high pressure BIVR decreases and the mass flow rate rises. The power output can therefore be increased by moving away from the maximum efficiency point, but it is important to choose the BIVR values so as to ensure that efficiency is maximised for a particular power output. Figure 8 shows that maximum net power output for any value of HP BIVR occurs at approximately constant LP BIVR values of around 3.6, and that this corresponds to the maximum cycle efficiency possible for a particular value of HP BIVR. It is therefore possible to plot curves for this range of conditions, showing the maximum values of total expander shaft power and adiabatic efficiency as functions of the mass flow rate. These are shown in Figure 9 along with the corresponding performance of single stage screw expanders with main rotor diameters of 145, 204 and 408mm for the same application. In all cases, the curves show the full range of performance achievable using the specified expander(s) within the practical range of BIVR values.

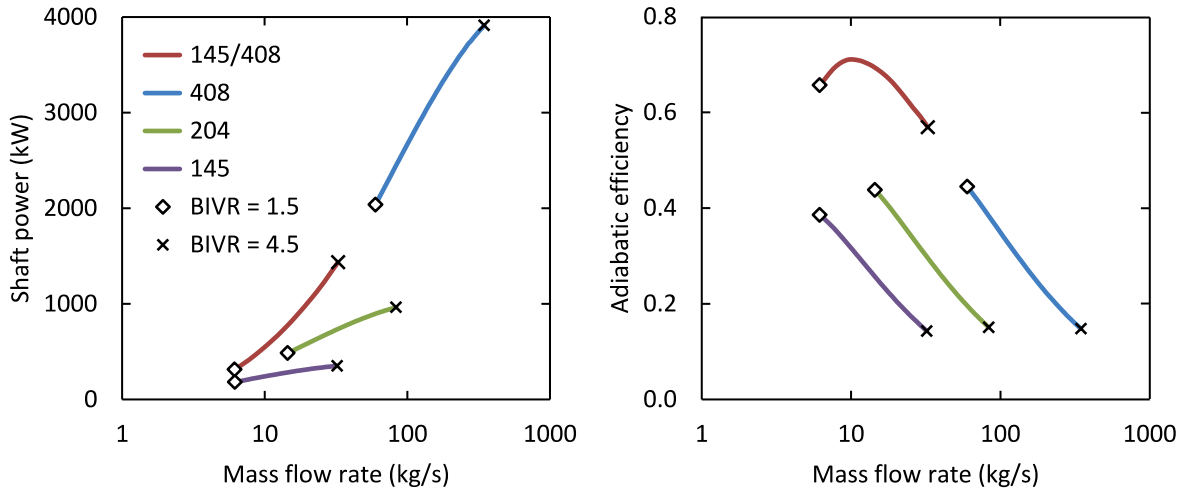

Figure 9: Performance comparison of single and 2-stage expanders with values of BIVR ranging between 1.5 and 4.5, when achieving maximum cycle efficiency as a function of net power output

The results in Figure 9 show that for single stage expanders, increasing the BIVR increases the efficiency, while the mass flow rate through the expander is reduced. For all of the single stage expanders considered, the maximum efficiency is well below 50% due to the large degree of under expansion. This is a result of the limited BIVR being much lower than the actual specific volume ratio of the working fluid over the expansion process. The two-stage machine achieves a much greater combined BIVR, and is therefore able to better match the overall expansion. The peak of the efficiency curve in Figure 9 shows the point where the expansion in the two-stage machine is best matched to the operating conditions. At higher mass flow rates the efficiency falls due to increasing under-expansion of the working fluid in both stages, while at lower mass flow rates it falls due to over-expansion in the LP stage. Interestingly, the results in Figure 9 suggest that a two-stage machine may be viewed as equivalent to the LP machine operating as a single stage but with a BIVR higher than the practical limit; this is illustrated by the fact that the shaft power and efficiency curves for the two-stage 145mm/408mm machine are essentially extensions of the performance curves for the single 408mm machine, covering a lower range of mass flow rates. It is also worth noting that, as the mass flow rate of the two-stage machine is largely a function of the BIVR of the HP stage, this range of achievable mass flow rate is very close to that of the single 145mm machine. In summary, compared to the LP stage operating alone, the addition of the HP stage can be seen to increase efficiency, but only by reducing mass flow rate and hence power output.

5. Results of Smith Cycle expander modelling

The results obtained for the high pressure expander in the 2-stage screw machine described in Section 4 can also be used to investigate the performance of the Smith Cycle for this application. As the pressure and the dryness fraction downstream of the HP expander are known, the mass flow rate of dry saturated vapour available for expansion in a LP turbine can be calculated. As the case being investigated imposes no lower temperature limit on the source fluid, recuperative feed heating offers no benefits in terms of power output, and has not therefore been considered. The separated liquid is therefore simply throttled to the condenser inlet pressure and mixed with the superheated vapour exiting the LP turbine. It should however be noted that in cases where the minimum allowable source temperature is significantly greater than the temperature of the working fluid at the feed pump exit, further investigation is required to determine whether the potential benefits of internal heat exchange are sufficient to justify the increased system complexity. Other than the calculated efficiency of the HP screw expander, the assumptions

described in Section 3 are again used to characterize the cycle. The resulting cycle efficiency and net power output are shown in Figure 11.

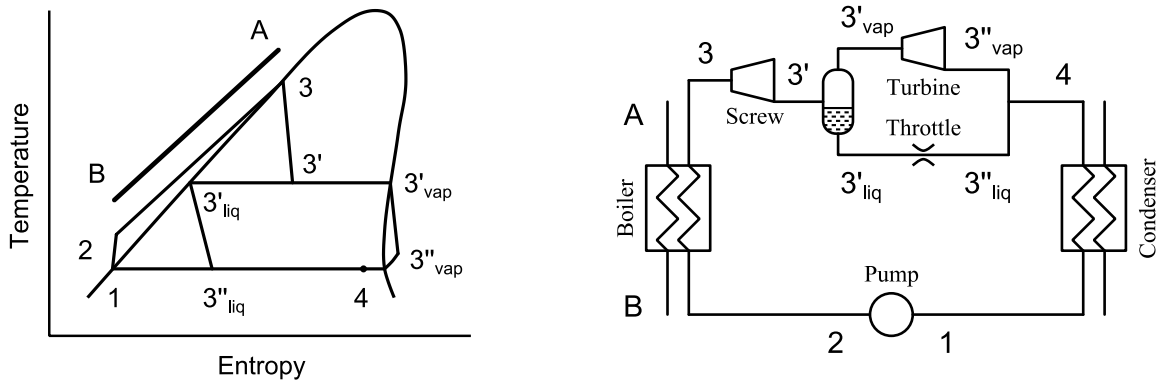

Figure 10: Temperature-entropy diagram and schematic diagram for simple Smith Cycle without recuperative or regenerative feed heating

The maximum cycle efficiency for the Smith Cycle is similar to that achieved in the TFC with 2-stage screw expander, and is seen to occur with BIVR = 4 for the high pressure screw machine and an intermediate pressure of around 5.5 bar. From Figures 4-6 it can be seen that at these conditions the working fluid is under-expanded in the high pressure screw machine, with $R_{dis} = 0.1$, and the resulting isentropic efficiency is around 70%. The required pressure ratio for the low pressure turbine is 5.5, which is at the top end of what can be achieved in a single-stage radial turbine. The relationship between BIVR and intermediate pressure values that result in maximum cycle efficiency for a given net power output can again be identified, as shown in Figure 11.

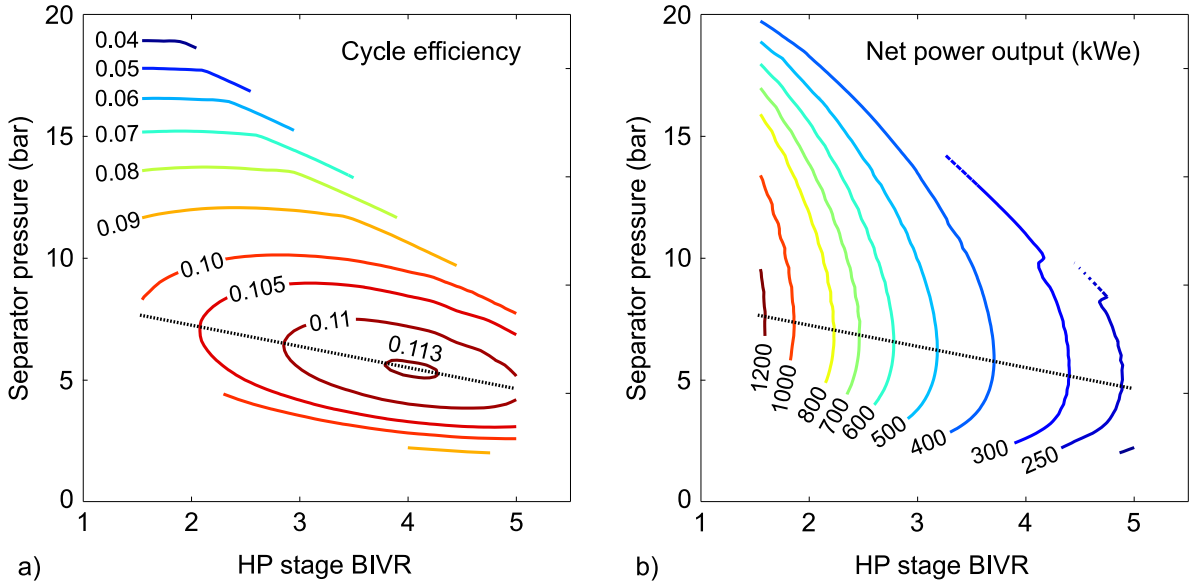

Figure 11: Contour maps showing a) Cycle efficiency and b) Net power output (kWe) for the Smith Cycle using a 145mm screw expander for the HP stage, where dashed lines show conditions required to maximise cycle efficiency as a function of net power output

6. Comparison of TFC, saturated ORC and Smith Cycle performance

It is clear from the results that the efficiency and mass flow rate of the screw expander affect the required power input and net power output of the systems with saturated liquid expansion. Two important measures of the overall system performance are the conversion efficiency, defined as the net power output divided by the *available* heat input, and the cycle efficiency, defined as net output power divided by the *actual* heat input. For the systems using screw expanders described in Sections 4 and 5, net power output is dependent on the mass flow rate, as this affects both the expander efficiency and work done in the feed pumps. The net electrical power output and the resulting overall conversion efficiencies of the 2-stage TFC and the Smith Cycle systems are shown in Figure 12. For comparison, the performance of TFC systems using only a single-stage screw expander with main rotor diameters of 145, 204 and 408mm are also shown. Finally, the conversion efficiencies calculated in Section 3.1 for the saturated vapour ORC systems using various working fluids are also shown, although the assumption of fixed turbine efficiency means that these results are independent of mass flow rate.

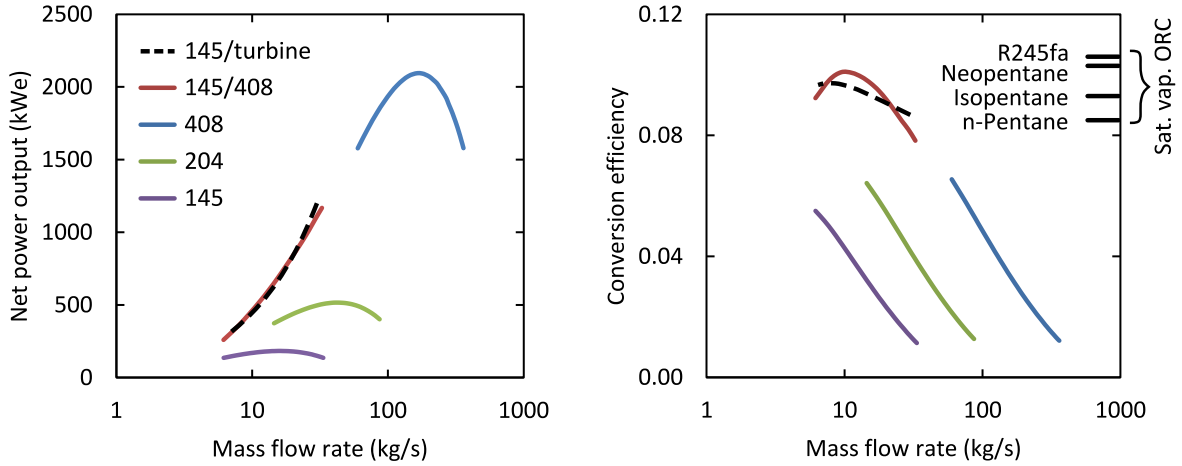

Figure 12: Achievable TFC net power output and conversion efficiency using TFC systems with single and two-stage expanders, and a Smith Cycle with 145mm HP screw and LP turbine

The results from Figure 12 suggest that in the range of system sizes covered by the TFC with two-stage expander (250-1200kWe) and the Smith Cycle using a single 145mm high pressure screw expander, the conversion efficiency is in a similar range to that which can be achieved in a simple saturated vapour ORC with two-stage turbine. This is largely due to the greater recovery of available heat from the source fluid, despite the lower predicted efficiency of the screw machines.

The TFC system achieves slightly higher maximum conversion efficiency than the Smith Cycle when a 145mm screw expander is used for the high pressure stage in both cases. The power output of TFC is limited by the required size of LP screw expander, which in practice means that the maximum rotor diameter is limited to around 0.5m due to manufacturing constraints. However, power output of the Smith Cycle is only limited by the required size of the HP screw expander. As the density of the working fluid is much greater in the HP stage, it is possible to implement cycles with much higher power output than is possible for the 2-stage TFC. For example, the use of a 408mm machine for the HP stage of the Smith Cycle (with the same tip speed limit of 60m/s) would increase the working fluid mass flow rate by a factor of around 8, leading to systems with net power outputs of up to 10 MWe. It is also likely that the isentropic efficiency of the larger machine would be higher due to the fact that manufacturing tolerances mean that clearance gaps do not increase linearly with rotor diameter, and leakages are therefore a lower proportion of the total mass flow rate.

7. Conclusions

The study presented in this paper shows that two-stage screw expanders can match the required volume ratio for the expansion of saturated liquid in waste heat recovery applications, and achieve high overall adiabatic efficiency. The design parameters for the two-stage machine can be optimised in order to maximize shaft power output for a given mass flow rate, and the possible range of operation of the two-stage machine has been mapped out. This allows a direct comparison of the performance of different single and two-stage machines operating under the same conditions. In the application discussed in this paper, the TFC using a two-stage expander and the Smith Cycle using a high pressure screw and low pressure turbine are both predicted to achieve a similar overall conversion efficiency to that of a conventional saturated vapour ORC. The choice of system for a particular application is therefore likely to be strongly influenced by other factors such as initial and operational costs, component design limitations, reliability, system control and off-design performance. Although not considered in the current study, ORC, TFC and Smith Cycle systems are all suitable for implementing regenerative and/or recuperative pre-heating of the feed liquid, and future work will investigate the application of these systems in cases where the source fluid is temperature limited. For a rigorous comparison of the systems considered here, more work is required to characterise achievable turbine efficiency for ORC applications with various working fluids and 2-stage expansion from saturated or superheated conditions. Another area for further study is the performance of the ORC, TFC and Smith Cycle systems at off-design conditions. This is of particular interesting in systems using screw expanders, as the ability to adjust the inlet dryness fraction and the BIVR (with a variable port design) may have advantages in terms of maximising energy production under varying heat source and heat sink conditions.

References

[1] House, P.A., Helical-rotor expander applications for geothermal energy conversion (No. UCRL-52043). California Univ., Livermore (USA). Lawrence Livermore Laboratory, 1976

[2] Elliot, D.G., Theory and tests of two-phase turbines (No. DOE/ER-10614-1; JPL-PUB-81-105). Jet Propulsion Lab., Pasadena, CA (USA); National Aeronautics and Space Administration, 1982

[3] DiPippo, R., Ideal thermal efficiency for geothermal binary plants. Geothermics, 2007, 36(3), pp.276-285.

[4] Smith, I.K., Stosic, N., Kovacevic, A., Power recovery from low cost two-phase expanders, Transactions of Geothermal Resource Council, 2001, p. 601-606.

[5] Smith, I.K., N Stosic, N., Kovacevic, A., Screw expanders increase output and decrease the cost of geothermal binary power plant systems, Transactions of Geothermal Resource Council, 2005, p. 25-28.

[6] Smith, I.K., Stosic, N., Aldis, C.A., Development of the Trilateral Flash Cycle System: Part 3: The Design of High-Efficiency Two-Phase Screw Expanders, Proceedings of the Institution of Mechanical Engineers, Part A: Journal of Power and Energy, 1996, 210(1): 75-93.

[7] Smith, I.K., Stosic, N., Kovacevic, A., Power Recovery from Low Grade Heat by Means of Screw Expanders, Elsevier, 2014

[8] Kane, M., Larrain, D., Favrat, D. and Allani, Y., Small hybrid solar power system. Energy, 2003, 28(14), pp.1427-1443.

[9] Bombarda, P., Invernizzi, C.M. and Pietra, C., Heat recovery from Diesel engines: A thermodynamic comparison between Kalina and ORC cycles. Applied Thermal Engineering,

2010, 30(2), pp.212-219.

[10] Taniguchi, H., Kudo, K., Giedt, W.H., Park, I. and Kumazawa, S., Analytical and experimental investigation of two-phase flow screw expanders for power generation. Journal of engineering for gas turbines and power, 1988, 110(4), pp.628-635.

[11] Tang, Y.; Fleming, J. S., Obtaining the optimum geometrical parameters of a refrigeration helical screw compressor. In 11th International Compressor Engineering Conference, Purdue University, 1992, pp 221-227.

[12] Fleming, J. S.; Tang, Y.; Xing, Z. W.; Cook, G., The Use of Superfeed in a Refrigeration Plant With a Twin Screw Compressor: an Optimization Technique for Plant Design. In Proceedings of the IIR XIXth Congress on Refrigeration, 1995, The Hague

[13] Fujiwara, M.; Osada, Y. , Performance analysis of an oil-injected screw compressor and its application. International Journal of Refrigeration, 1995, 18, (4), 220-227

[14] Stosic, N., Hanjalic, K., Development and Optimization of Screw Machines with a Simulation Model - Part I: Profile Generation, Journal of Fluids Engineering, 1997, 119(3): 659-663.

[15] Hanjalic, K., Stosic, N., Development and Optimization of Screw Machines with a Simulation Model - Part II: Thermodynamic Performance Simulation and Design Optimization, Journal of Fluids Engineering, 1997, 119(3): 664-670.

[16] Smith, I.K., Stosic, N., Aldis, C.A., Development of the Trilateral Flash Cycle System: Part 3: The Design of High-Efficiency Two-Phase Screw Expanders, Proceedings of the Institution of Mechanical Engineers, Part A: Journal of Power and Energy, 1996, 210(1): 75-93.

[17] Read, M.G., Stosic, N., & Smith, I. K., Optimization of Screw Expanders for Power Recovery From Low-Grade Heat Sources, Energy Technology & Policy, 2014, 1(1), 131-142.

[18] Sakun, I.A. *Screw Compressors*; Mashgiz Press: Moscow, Russia, 1960. (In Russian)

[19] Uusitalo, A. Working Fluid Selection and Design of Small-Scale Waste Heat Recovery Systems Based on Organic Rankine Cycles. Ph.D. Thesis, Acta Universitatis Lappeenrantaensis, Lappeenranta University of Technology, Finland, 2014

[20] Da Lio L, Manente G, Lazzaretto A. New efficiency charts for the optimum design of axial flow turbines for organic Rankine cycles. Energy. 2014, 77, 447–459.

[21] Kang, S.H. Design and experimental study of ORC (organic Rankine cycle) and radial turbine using R245fa working fluid. Energy. 2012, 41, 514–524.

[22] Calm, J.M., Comparative efficiencies and implications for greenhouse gas emissions of chiller refrigerants. International Journal of Refrigeration, 2006, 29(5), pp.833-841.